

THE UNIVERSITY OF MICHIGAN  
INDUSTRY PROGRAM OF THE COLLEGE OF ENGINEERING

INTERACTION EXPERIMENTS OF LATERAL  
JETS WITH SUPERSONIC STREAMS

James L. Amick  
Associate Research Engineer

Gerard F. Carvalho  
Research Assistant

Hans P. Liepman  
Associate Professor of Aeronautical Engineering and  
Supervisor of Supersonic Wind Tunnel

March, 1959

IP-361







## TABLE OF CONTENTS

	<u>Page</u>
LIST OF FIGURES.....	iii
INTRODUCTION.....	1
MODEL AND TEST EQUIPMENT.....	2
EXPERIMENTAL RESULTS.....	7
THEORETICAL CONCEPT.....	14
SUMMARY.....	18



# LIST OF FIGURES

<u>Figure</u>		<u>Page</u>
1	Exploded View of Side Jet Model.....	3
2	Exploded View of Side Jet Sting Balance.....	3
3	Windshield Effect on Single Jet Interaction.....	4
	a) large windshield (57-9-19-17) $P_{oj}/P_1 = 540$ .....	4
	b) small windshield (58-8-27-24) $P_{oj}/P_1 = 602$ .....	4
4	a) 2 Jets @ $30^\circ$ , $P_{oj}/P_1 = 410$ (58-8-28-12).....	8
	b) 3 Jets @ $30^\circ$ , $P_{oj}/P_1 = 366$ (58-8-26-9).....	8
	c) 4 Jets @ $30^\circ$ , $P_{oj}/P_1 = 370$ (58-8-25-38).....	9
	d) Slot ( $90^\circ$ ), $P_{oj}/P_1 = 420$ (58-8-23-21).....	9
5	a) Inclined Jet $15^\circ$ , $P_{oj}/P_1 = 409$ (58-8-27-16).....	10
	b) Inclined Jet $45^\circ$ , $P_{oj}/P_1 = 409$ (58-8-27-5).....	10
6	Normal Force Magnification Factor K.....	12
7	Normal Force Effectiveness Factor E.....	13
8	Two-Dimensional Side Jet Theory.....	15

NOTE: The numbers in parentheses denote the test run number.



## INTRODUCTION

Early in 1957 the University of Michigan started a modest research program on jet reaction controls for the Applied Physics Laboratory under Bureau of Ordnance sponsorship. The program consists of theoretical and experimental studies of missile control, stabilization, and sustentation by means of jets exhausting laterally from a typical missile.

Items of specific interest in this research program are:

1. The prediction of combined effects of two-or more radial jets at right angles to the surface of the missile.
2. The prediction and utilization of axial and radial components of inclined jets for purposes of stability, control, and sustentation.
3. The effects of forward jet locations.
4. Special jet reaction studies, such as the rolling due to tangential components of one or more jets.

Highlights of the results obtained to date are presented in this report.



## MODELS AND TEST EQUIPMENT

The experimental portions of the side-jet program are conducted in the 8 by 13 inch, atmospheric-to-vacuum, supersonic wind tunnel of the University's Aeronautical Engineering Laboratories. The Mach number 3.9 nozzle was used in all tests. Some of the earlier side-jet studies, however, had utilized the Mach 2.84 nozzle.

The model consists of a 2-inch-diameter cylindrical afterbody with interchangeable ogive-cylinder forebodies. The afterbody itself was made of three parts, the adapter to hold the forebodies, interchangeable cylindrical spacers for the various jet orifice geometries, and a base section to admit the jet gas and to serve as attachment to the hollow strain gauge sting. Figure (1) shows the various parts of the model while Figure (2) gives the details of the sting balance. The tapered windshield shown in Figure (2) was subsequently replaced by a smaller windshield of constant diameter. The tapered and larger windshield was suspected of influencing the pressures over the rear of the model and promoting premature boundary layer separation. The use of the smaller windshield did reduce such extraneous effects noticeably (see Figure 3).

The following jet orifice configurations have been tested to date;

1. Single orifices, normal to the surface with sharp and rounded entrance edges,  $.254D$  upstream of Base, where  $D$  is the model diameter.



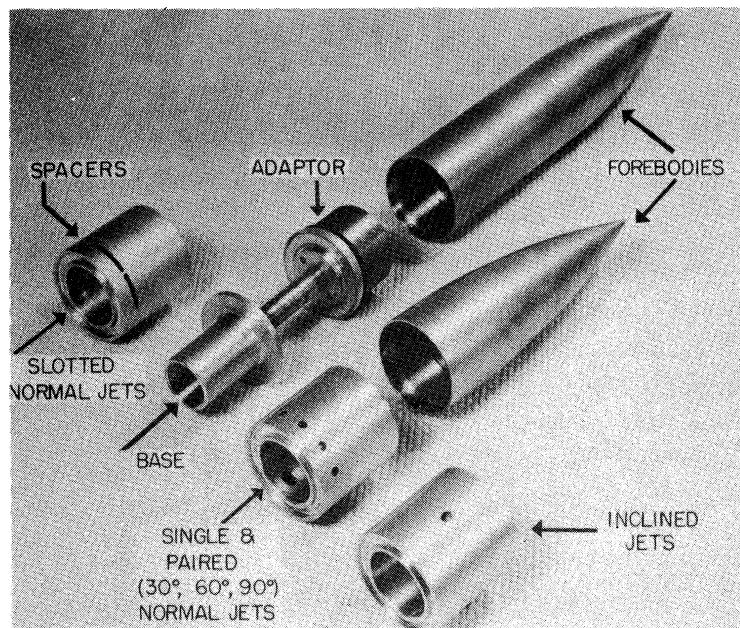


Figure 1. Exploded View of Side Jet Model.

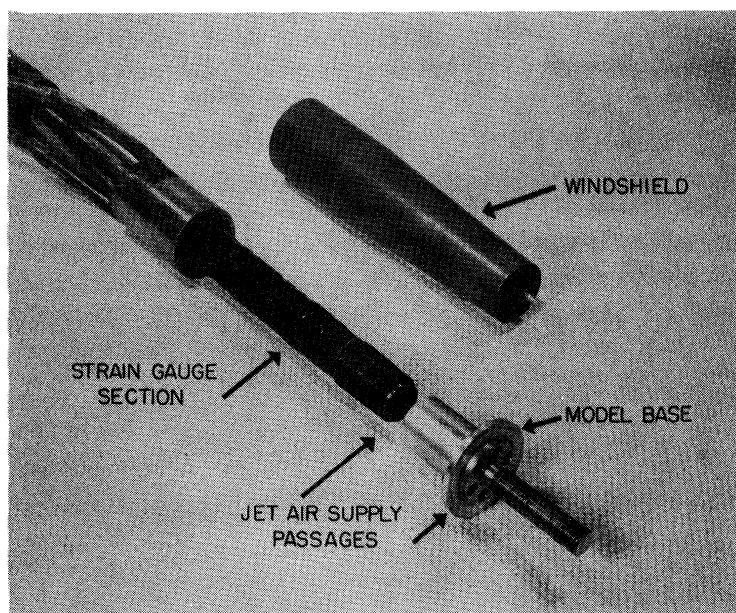
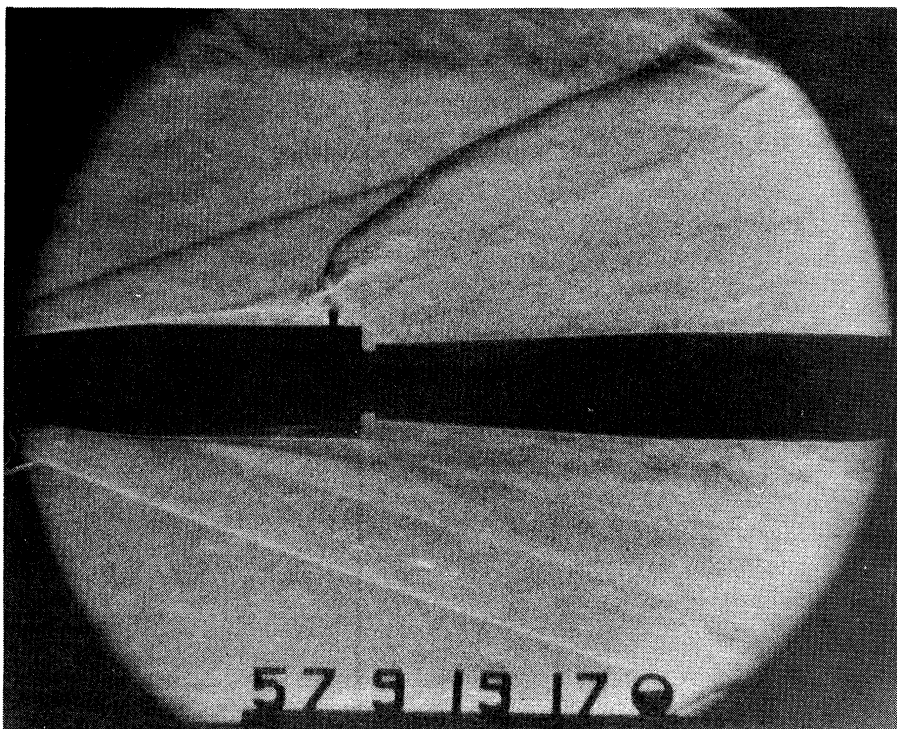
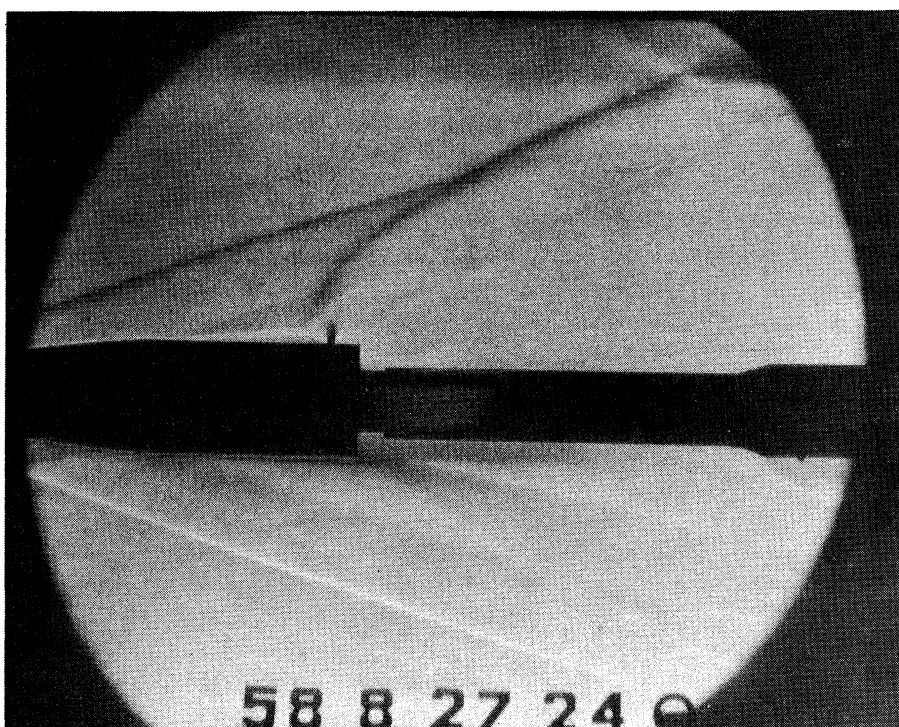


Figure 2. Exploded View of Side Jet Sting Balance.





a) Large Windshield,  $P_{Oj}/P_1 = 540$ .



b) Small Windshield,  $P_{Oj}/P_1 = 602$ .

Figure 3. Windshield Effects on Single Jets at  
 $M_1 = 3.9$ ,  $P_1 = .107$  psia.



2. Single round-edged orifices inclined forward  $15^\circ$ ,  $30^\circ$ , and  $45^\circ$ ,  $.565D$  upstream of base.
3. Twin, sharp-edged, normal orifices at  $30^\circ$ ,  $60^\circ$ , and  $90^\circ$  circumferential spacing,  $.254D$  upstream of base.
4. Three normal orifices at  $30^\circ$  spacing,  $.254D$  upstream of base.
5. Four normal orifices at  $30^\circ$  spacing,  $.254D$  upstream of base.
6. Narrow slot, normal to axis, over  $90^\circ$  circumference,  $.254D$  upstream of base.
7. Single nose jet on long forebody, normal to surface,  $.611D$  downstream of nose.

All orifices employed so far were sonic and had nominal diameters of 0.159 inches, while the slot was  $3/32$ " wide.

The jet gas used was laboratory air and the jet stagnation pressure was varied from about 1 psia to 125 psia by means of Grove regulators. Earlier tests with a similar model had shown that the jet stagnation temperature remained essentially constant over the entire pressure range. Normal forces and centers of pressure of the models were measured by a two-component balance. The model set-up in the tunnel proper was also used to obtain the reference jet reaction ( $N_V$ ) by operating the jet into the fully evacuated (about .1 psia) tunnel. The normal force measured in that manner was taken to be the jet reaction force in a vacuum ( $N_V$ ) of each orifice which was always



less than the theoretical jet force in a vacuum ( $N_{vth}$ ) due to the internal geometry of each orifice.

Schlieren pictures were taken to observe the jet effects on the boundary layer and to give an idea of the flow field around the body. Almost all recent schlieren pictures have been taken with steady light and a 1/50 sec. exposure, instead of the usual 5-micro-second spark exposures of which Figure (3a) is the only example in this report. The 1/50 sec. exposure gives essentially a time average of the flow which is more indicative of the jet structure and the unsteadiness of the jet bow wave.

The boundary layer on all models tested at  $M = 3.9$  was laminar. No attempt was made to induce a turbulent layer by means of trippers. Earlier tests with both types of boundary layers indicated that the total normal force due to aft jets did not depend on the character of the boundary layer.



## EXPERIMENTAL RESULTS

The highlights of the results obtained to date are collected in this part. Some of the data must be taken as preliminary until the detailed review of the experimental results, the calibration data, and the data reduction process, has been completed. This word of caution applies to the nose-jet data and the inclined aft-jets.

Representative schlieren pictures of several jet configurations exhausting into a Mach 3.9 flow are shown in Figures (3) to (5). The configuration of each jet and its operating condition is given on each schlieren picture. The extent of the jet-body interaction field is evidenced by the upstream location of the boundary layer separation around the model.

The results from the strain gauge balance are summarized in Figures (6) and (7) in terms of a normal force magnification factor  $K$  and a normal force effectiveness factor  $E$ , respectively. These factors are defined as

$$K = N_{\Delta}/N_v \quad (1)$$

$$E = N_{\Delta}/T_{vth} \quad (2)$$

where

$$N_{\Delta} = (\text{Normal Force})_{\text{jet on}} - (\text{Normal Force})_{\text{jet off}}$$

$$N_v = (\text{Normal Force in Vacuum})_{\text{jet on}}$$

$$\begin{aligned} T_{vth} &= \text{Theoretical Jet thrust in Vacuum} \\ &= 2 [2/(\gamma + 1)]^{1/(\gamma - 1)} P_{oj} A_j. \end{aligned}$$

The magnification factor for single aft jets is seen to be of significant magnitude (Figure 6a), varying from 1.50 to 1.70 at  $P_{oj}/P_1$



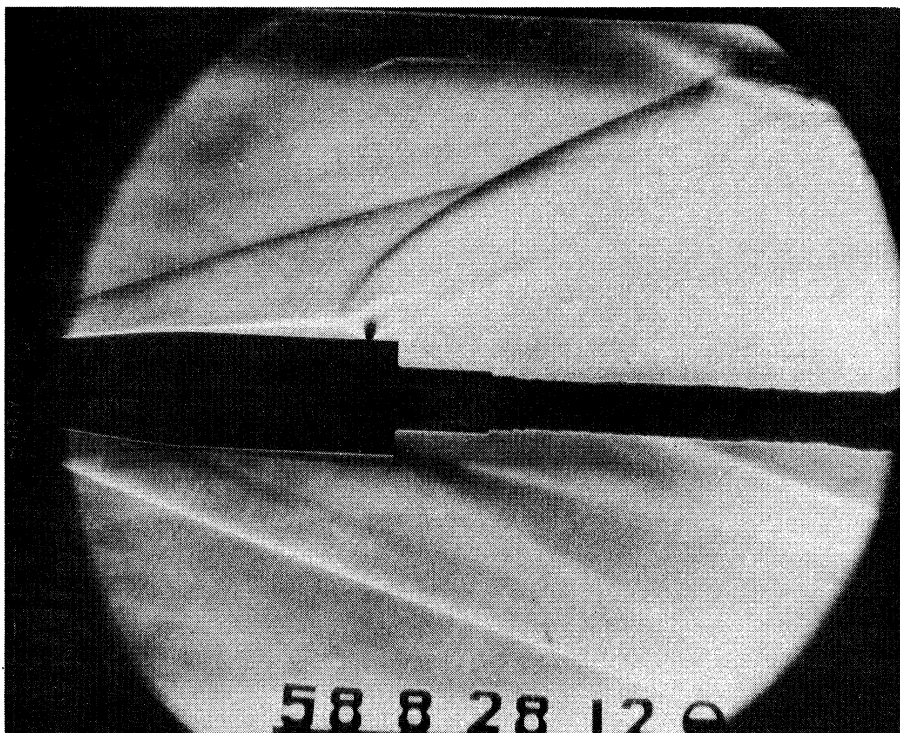


Figure 4a. Two Jets at 30° Circumferential Spacing,  
 $P_{oj}/P_1 = 410$ ,  $M_1 = 3.9$ ,  $P_1 = .107$  psia.

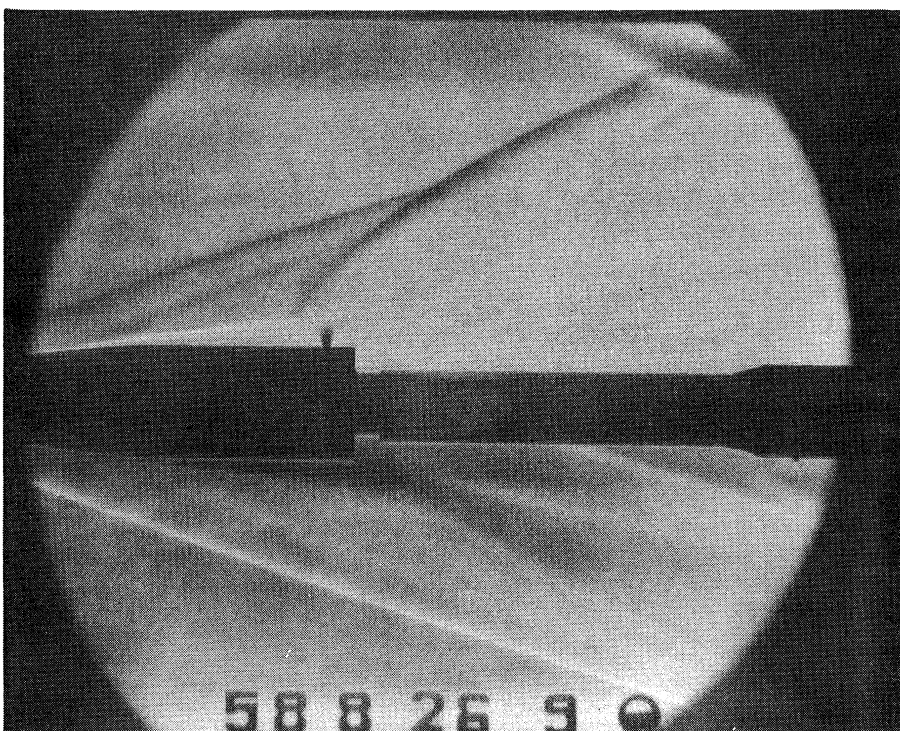


Figure 4b. Three Jets at 30°,  $P_{oj}/P_1 = 366$ .



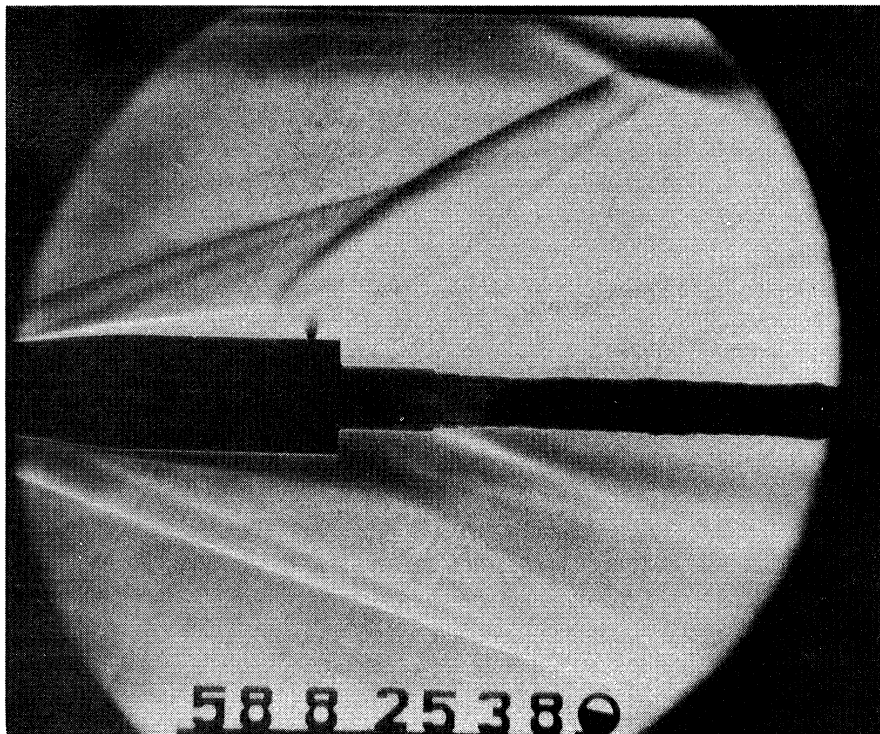


Figure 4c. Four Jets at  $30^\circ$ ,  $P_{oj}/P_1 = 370$ .

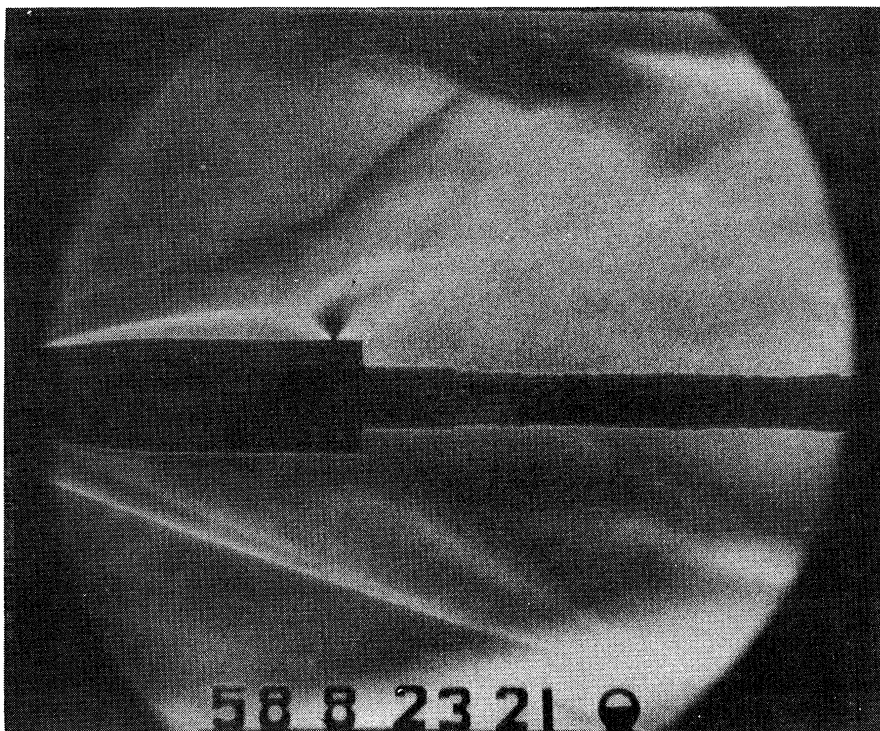


Figure 4d. Slot Over  $90^\circ$ ,  $P_{oj}/P_1 = 420$ .



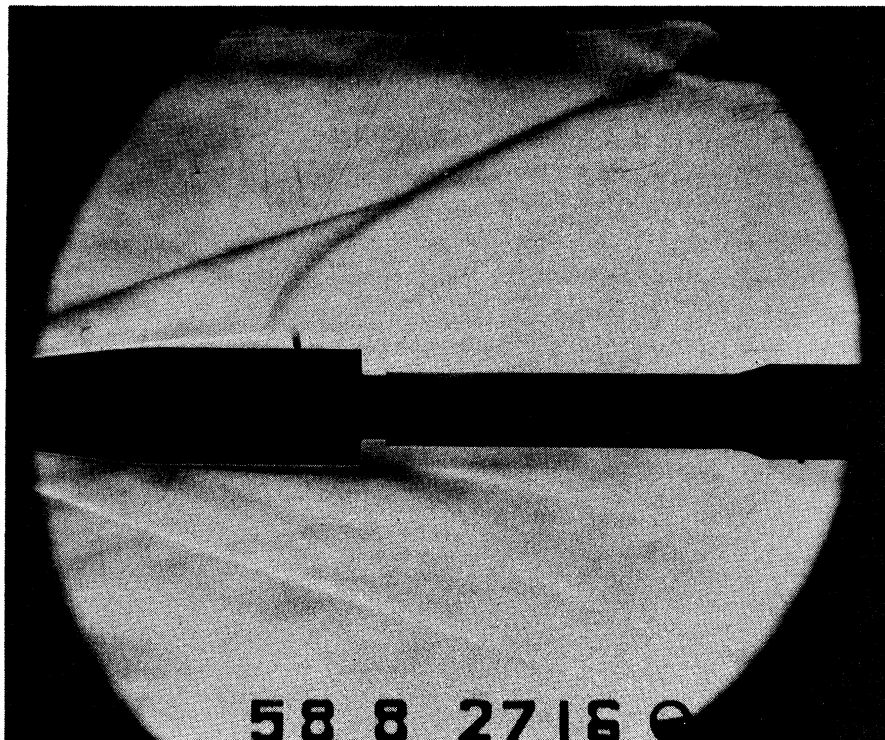


Figure 5a. Single Jet Inclined  $15^\circ$  Forward  
 $P_{0j}/P_1 = 400$ ,  $M_1 = 3.9$ ,  $P_1 = .107$  psia.

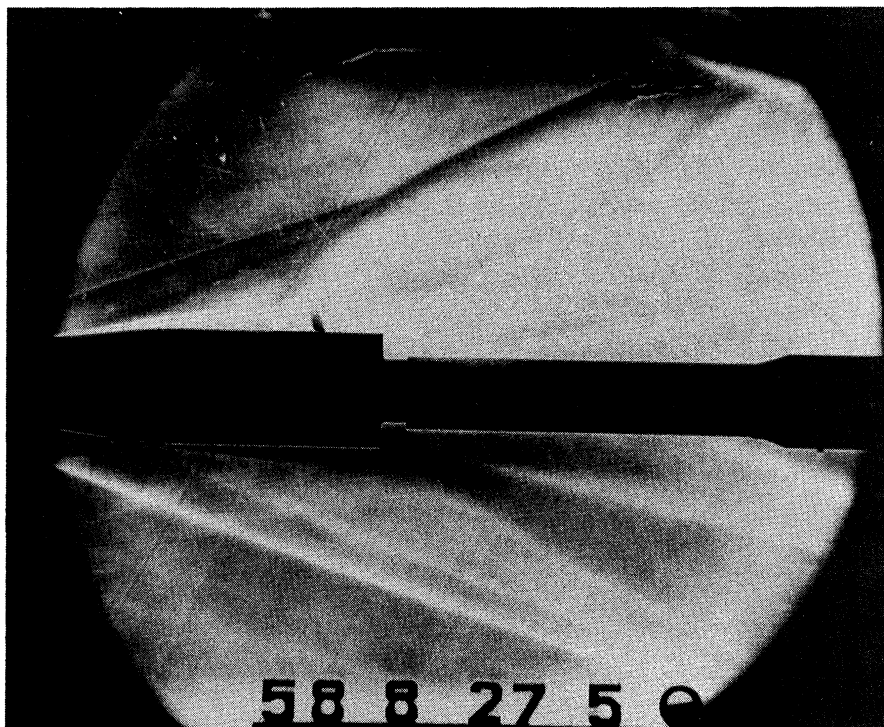


Figure 5b. Single Jet Inclined  $45^\circ$  Forward  
 $P_{0j}/P_1 = 400$ .



of 100 to 1.1 to 1.3 at a pressure ratio of 1000. The slightly lower magnification factors for the inclined jets shown are reasonable, since these orifices are further upstream of the base than the straight ones. Tests of aft-inclined jets and studies of the flow field are planned for the next phase.

The preliminary curve for the nose jet shows poor performance at low pressure ratios, but rises to full theoretical force ( $K = 1$ ) above  $P_{Oj}/P_1 = 500$ . It is planned to explore this aspect in more detail by moving the model sufficiently far back so that the flow field around the nose and the jet becomes visible.

The performance of the multiple jets shown in Figure (6b) is less than that of the single jets and decreases in a reasonable manner as the number of orifices increases.

The normal force effectiveness (Figure 7) seems to be about the same for all single aft jets, both normal and inclined ones, while the nose jet appears to be considerably poorer. Multiple jets are less effective than single jets.

Considering the normal force aspects of side jets one notes that aft-jets do realize a sizeable and helpful interaction effect which may well be useful for practical applications at intermediate altitudes where finite densities are available.

Further work is needed, however, especially on the question of drag, to arrive at an evaluation of the overall side jet effectiveness. This is planned for the continuation of this program.



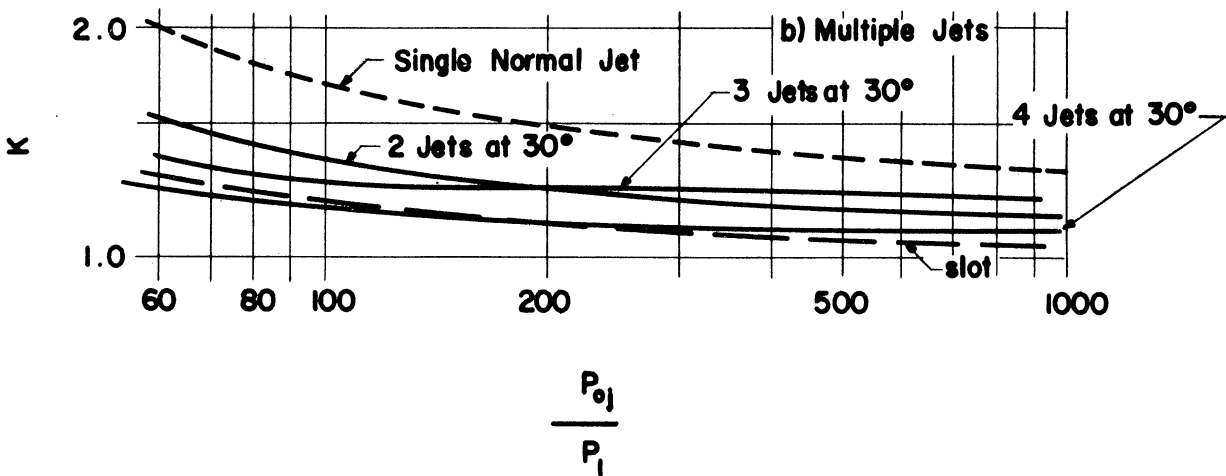
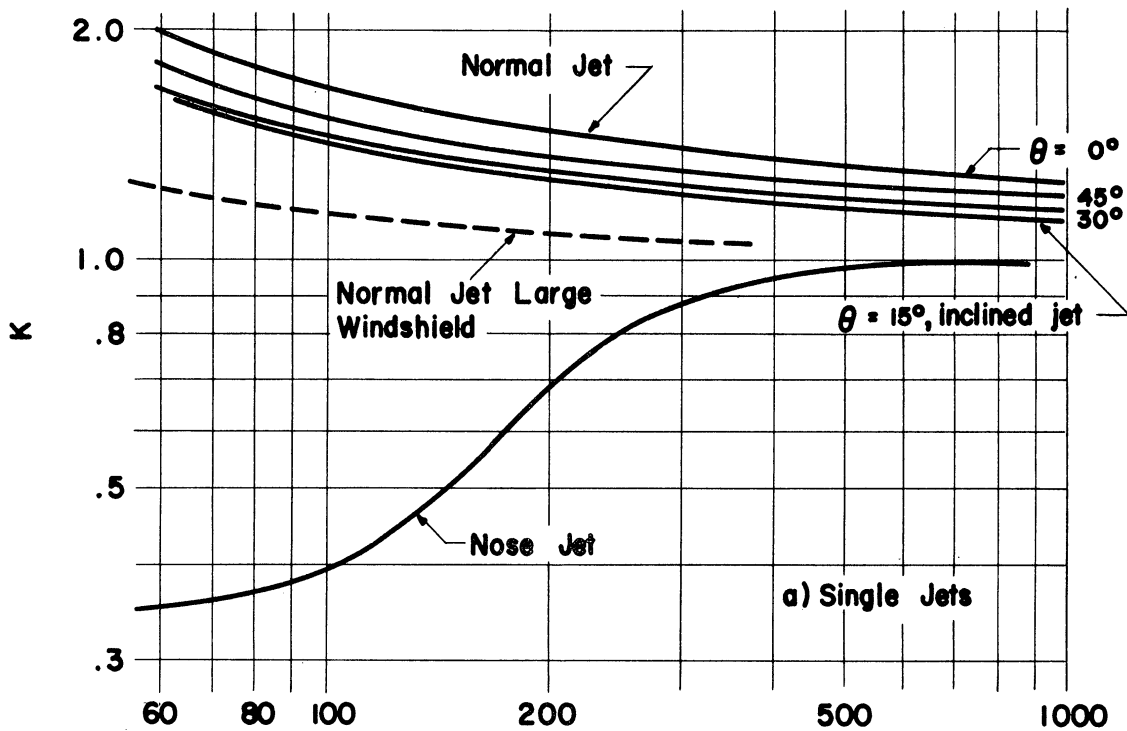
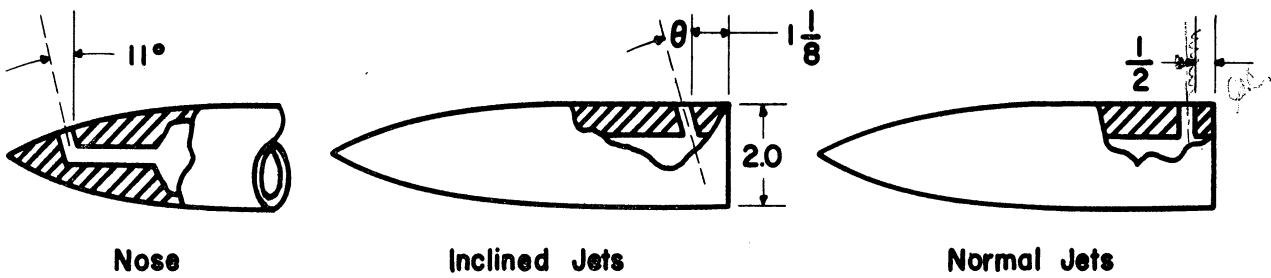


Figure 6. Normal Force Magnification Factor Versus Jet Stagnation Pressure Ratio.  $M = 3.9$ ,  $P_1 = .107$  Psia. Small Windshield Except Where Noted.



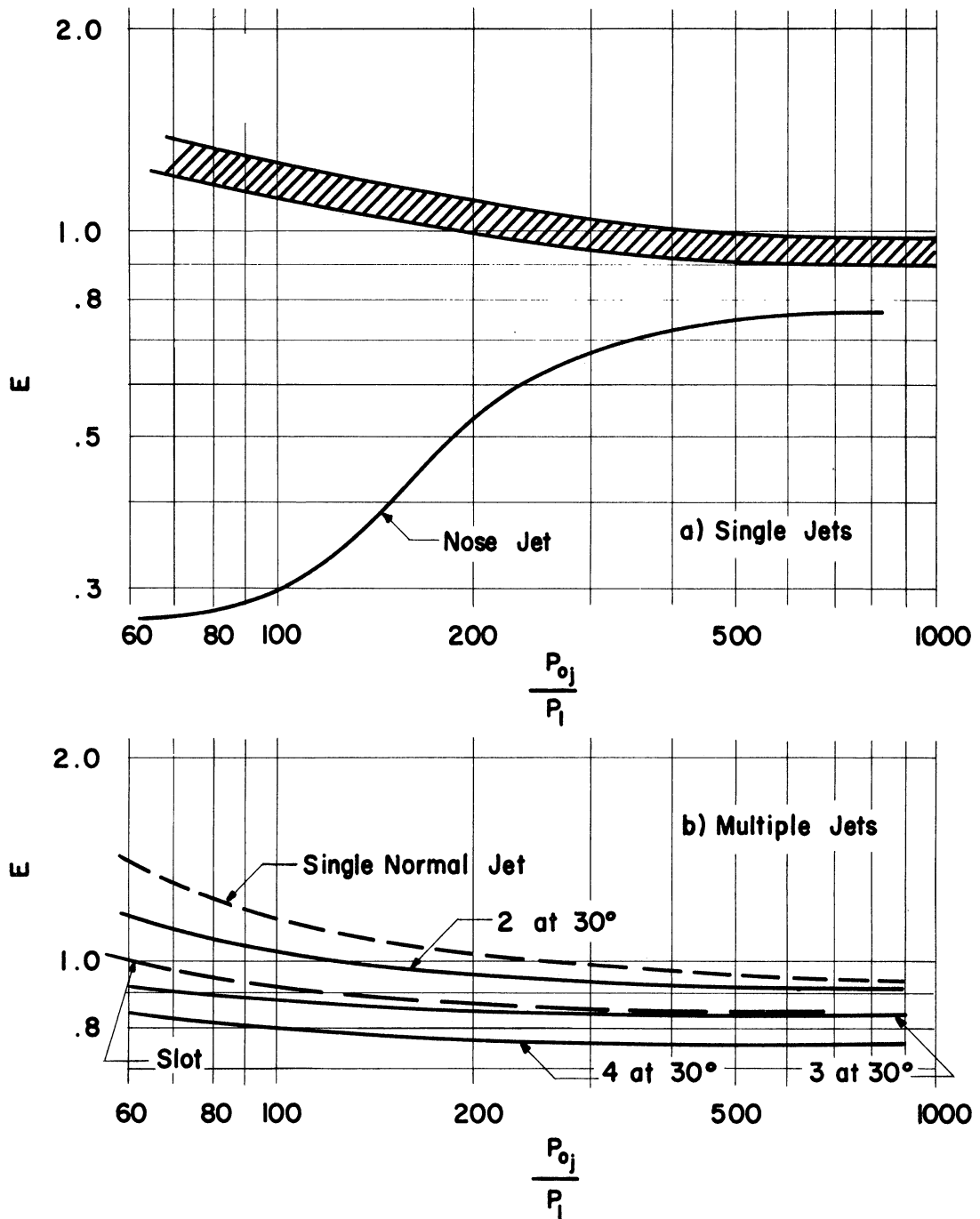


Figure 7. Normal Force Effectiveness Factor Versus Jet Stagnation Pressure Ratio.  $M = 3.9$ ,  $P_1 = .107$  Psia. Small Windshield.



### THEORETICAL CONCEPTS

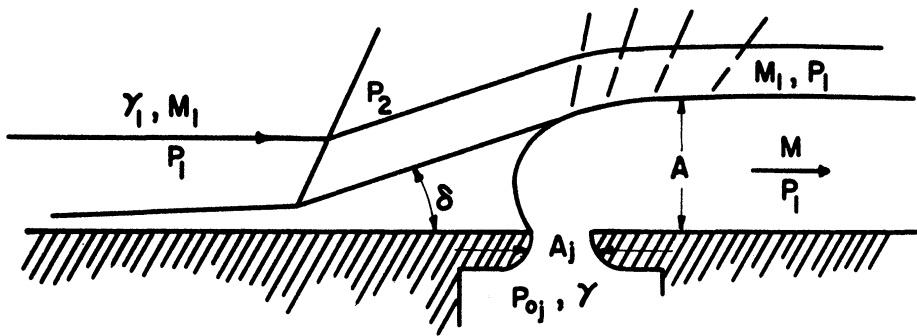
Even the simplest theoretical model is of great value in interpreting experimental results. A simplified analysis was, therefore, made sometime ago of the interaction of a two-dimensional side-jet with a supersonic main stream. The jet is assumed to expand isentropically to the free stream static pressure, turning at the same time to flow downstream along the surface of the body (Figure 8). The thickness of the jet after expanding and turning acts as a spoiler of height  $A$  which separates the boundary layer and forces the main flow to compressively turn through an angle  $\delta$  upstream of the jet.

From this theoretical model, one can derive an expression for the interaction force  $N_I$  which is defined as

$$N_I = N_{\Delta} - N_V \quad (3)$$

The normal force for any flow condition can be written as the sum of two components, one the resultant of all pressures acting on the outside of the body, the other the resultant of all internal pressures. In a vacuum, then, the component due to external pressures is essentially zero, so that  $(N_{int.})_V = N_V$ . For a supersonic jet, exhausting into an airstream (finite ambient pressure), the normal force component due to internal pressures is still equal to  $N_V$  because the sonic throat of the jet prevents external pressures from communicating with the inside. With the jet turned off, the internal pressure becomes equal to the ambient pressure  $P_1$ , so that the internal normal force is just  $P_1 A_j$ , with  $A_j$  denoting the throat area of the jet.





$$\frac{N_I}{N_V} = \frac{\gamma_1 M_1^2}{2 \left\{ \frac{\gamma+1}{\gamma-1} (M_1^2 - 1) \left[ \left( \frac{P_{0j}}{P_1} \right)^{\frac{\gamma-1}{\gamma}} - 1 \right] \left( \frac{P_{0j}}{P_1} \right)^{\frac{\gamma-1}{\gamma}} \right\}^{1/2}} - \left[ 2 \left( \frac{2}{\gamma+1} \right)^{\frac{1}{\gamma-1}} \left( \frac{P_{0j}}{P_1} \right) \right]^{-1}$$

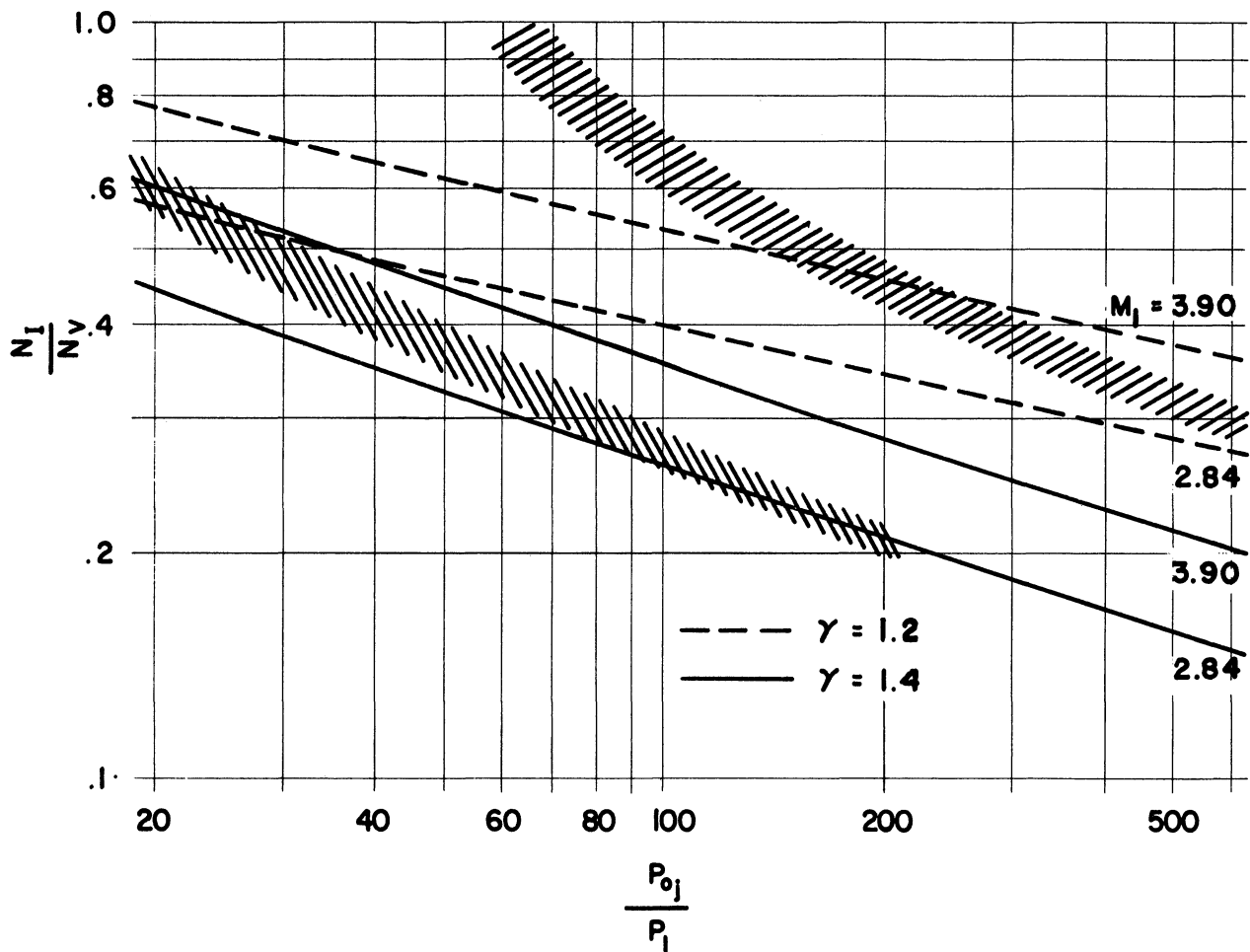


Figure 8. Two-Dimensional Side - Jet Theory.



The difference in normal force due to internal pressures for jet-on and jet-off conditions is therefore

$$(N_{\Delta})_{\text{int}} = N_v - P_1 A_j . \quad (4)$$

The interaction force can now be written as

$$N_I = (N_{\Delta})_{\text{ext}} - P_1 A_j . \quad (5)$$

$(N_{\Delta})_{\text{ext}}$ , the difference in normal force due to external pressures between jet-on and jet-off conditions, is from the sketch of Figure (8),  $(N_{\Delta})_{\text{ext}} = (P_2 - P_1) A / \tan \gamma$ . (6)

Substitution of the familiar expressions

$$P_2/P_1 = 1 + \gamma_1 M_1^2 \delta / (M_1^2 - 1)^{1/2}$$

$$\tan \delta = \delta,$$

$$A/A_j = (2/\gamma+1)^{\frac{\gamma+1}{2(\gamma-1)}} \frac{(P_{Oj}/P_1)^{\frac{\gamma+1}{2\gamma}}}{\sqrt{\frac{2}{\gamma-1} \left[ (P_{Oj}/P_1)^{\frac{\gamma-1}{\gamma}} - 1 \right]}}$$

$$N_v = 2P_{Oj} A_j (2/\gamma+1)^{\frac{1}{\gamma-1}},$$

into Equations (5) and (6) results in the following expression for the ratio of the interaction force to the jet force in a vacuum:

$$N_I/N_v = \frac{\gamma_1 M_1^2}{2 \sqrt{\frac{\gamma+1}{\gamma-1} (M_1^2 - 1) \left[ (P_{Oj}/P_1)^{\frac{\gamma-1}{\gamma}} - 1 \right] (P_{Oj}/P_1)^{\frac{\gamma-1}{\gamma}}}} - \frac{1}{2 \left( \frac{2}{\gamma+1} \right)^{\frac{1}{\gamma-1}} (P_{Oj}/P_1)}$$

(Note that by definition  $N_I/N_v = (N_{\Delta}/N_v) - 1 = K-1$ )

The results of the above theory are shown in Figure (8) for Mach number 2.84 and 3.9 and for two jet gases with  $\delta$ 's of 1.2 and 1.4.

The shaded areas represent experimental data at the two Mach numbers with air as the jet medium.



A more refined theoretical analysis of a two-dimensional side-jet utilizes the method of characteristics to find the shape of the jet for a given stagnation pressure, free stream and exit Mach numbers, and judiciously assumed pressures upstream and downstream of the jet.

The interaction forces calculated from such a physical model turned out to be about an order of magnitude higher than those of the simple theory. In this example the jet exit and free stream Mach numbers were 4.0, the upstream pressure was determined from laminar separation and reattachment conditions, and the downstream pressure was assumed to be three tenths of ambient pressure.



# SUMMARY

The results presented here can be summarized as follows:

1. All aft-jets tested, single as well as multiple ones, show significant normal force magnification factors for all jet-stagnation-to-ambient pressure ratios.
2. All single aft-jets normal to the axis of the missile had about the same high normal force effectiveness.
3. The preliminary nose jet data show a normal force deficiency at low pressure ratios changing to unit magnification at the higher pressure ratios.
4. More basic data is needed for the nose jet to understand its behavior and to determine its effects on forebody drag.
5. A simple, two dimensional, theory for the normal force magnification seems to predict trends and approximate magnitudes for aft-jets but fails in case of the nose-jet.





THE UNIVERSITY OF MICHIGAN

DATE DUE

11/3 17:34